Characterization of the Mixture Formation Process in a GDI Engine Operating under Stratified Mode

L. Allocca*, M. Costa, A. Montanaro, P. Sementa, U. Sorge, B.M. Vaglieco
CNR - Istituto Motori, Naples, Italy
l.allocca@im.cnr.it, m.costa@im.cnr.it, a.montanaro@im.cnr.it,
p.sementa@im.cnr.it, u.sorge@im.cnr.it, b.m.vaglieco@im.cnr.it

Abstract

The paper is intended at an experimental and a numerical study of the mixture formation process in a GDI engine equipped with a high-pressure seven-hole injector. One of the 4 engine cylinders is modified to allow two optical accesses that leave unvaried the combustion chamber configuration, hence the performance and emissions of the real engine. A first optical access is through the piston head and a second one is through an endoscopic fiber probe inserted in the cylinder head. Under a medium-speed, medium-load working condition, the gasoline injection phase is experimentally characterized by image acquisition with high temporal resolution.

The considered injector is also preliminary experimentally characterized as delivering gasoline into an optically accessible confined vessel under various injection strategies. Spray images are collected to derive information relevant to penetration length and cone angle. The issuing mass flow rate is measured by means of a Bosch tube. The measurements data base is used to develop a 3D numerical model of the spray dynamics, whose validation is performed through an automatic procedure. The spray model is included within a 3D model of the in-cylinder processes to realize a reliable description of mixture formation and combustion.

Introduction

A way to significantly improve the energetic efficiency of internal combustion engines without making a major shift away from conventional technologies is well recognized in the use of direct injection (DI). In spark ignition (SI) engines, in particular, gasoline direct injection (GDI) is today considered indispensable to decrease fuel consumption, hence CO_2 emissions, as coupled with downsizing and turbo-charging. Thanks to the more precise control of the injection timings feasible through DI, well known limits of the port fuel injection (PFI) engines in the combustion control and fuel supply response are overwhelmed. These limits mainly consist in the throttle load control, the knock tendency under low speed/high load conditions, the stoichiometric operation of the engine required by the three-way exhausts after-treatment system, and the high unburned hydrocarbon (HC) and nitrogen mono-oxide (NO) emissions at the exhaust. Tendency to knock forces to lower the compression ratio of the engine, throttle load control and stoichiometric operation significantly increase the fuel consumption of the engine, whereas high HC and NO emissions remain a minor problem, due to the high efficiency of the generally employed three-way catalysts mounted at the exhaust [1, 2].

The GDI technology, especially with the employment of new generation high-pressure injectors in the multi-hole configuration, has the great advantage of improving the mixture formation process, with a positive effect on combustion stability and pollutants formation. Knock tendency is also favorably affected due to the decrease of the charge temperature consequent the in-cylinder gasoline evaporation. Nevertheless, due to the complexity of modern engines, assuring optimal mixture conditions at all the engine loads and speeds remains a difficult task, affected by different variables whose effects are strongly related. Recently, the capability of numerical techniques to achieve a complete control of the mixture formation process over the whole engine working map, to increase fuel economy, improve combustion stability and reduce engine-out emissions is being pursued [3, 4]. Two main aspects are of great relevance and need further study: from one hand the development of accurate models for the prediction of the in-cylinder spray dynamics, from the other, the use of advanced computational techniques that may assure that the engine is fed with the desired gasoline mass and timing as the in-chamber thermo-fluidynamic conditions vary.

Present work is aimed at a synergic numerical and experimental study of the mixture formation process in a GDI engine equipped with a high-pressure multi-hole injector. The study starts with an experimental characterization of the engine, aimed to collect both in-cylinder pressure data and images of the in-chamber spray development. One of the four engine cylinders has two optical accesses, one in the cylinder head, the other in the piston head [5].

* Corresponding author: l.allocca@im.cnr.it

The employed multi-hole injector is preliminary experimentally characterized both as generating sprays within an optically accessible vessel, and on a Bosch tube, to recover a precise measure of the delivered instantaneous mass flow rates. Collected data are employed as a database for the development and the validation of a 3D model for the spray dynamics. The spray model is included within a 3D model of the in-cylinder processes, able to simulate the whole engine working cycle. Main results of the 3D engine simulation are presented with reference to a medium-speed medium-load operating condition, with comparisons between experimental and numerical data relevant to both the in-cylinder pressure and the spray evolution.

Experimental Apparatus and Procedures

The experimental apparatus for the characterisation of the engine performance includes the following modules: the spark ignition engine, an electrical dynamometer, the fuel injection line, the data acquisition and control units, as well as the emission measurement system. The electrical dynamometer allows the engine operation under both motored and firing conditions.

Engine

The engine under study is a SI DI, inline 4-cylinder, 4-stroke, displacement of 1750 cm^3, turbocharged, high performance engine. It has a wall guided injection system with a seven-hole injector located between the intake valves and oriented at 70° with respect to the cylinder axis. The engine is equipped with a variable valve timing (VVT) system in order to optimize intake and exhaust valve lift for each regime of operation. The engine is not equipped with after-treatment devices. Further details of the engine are reported in Table I.

Table I Engine specifications

Unitary displacement [cm^3]	435.5
Bore [mm]	83
Stroke [mm]	80.5
Turbine	Exh. gas turbocharger
Max. boost pressure [bar]	2.5
Valve timing	Intake and exhaust VVT
Compression ratio	9.5:1
Max. power [kW]	147.1 @ 5000 rpm
Max. torque [Nm]	320.4 @ 1400 rpm

An optical shaft encoder is used to transmit the crank shaft position to the electronic control unit. The information is in digital pulses. The encoder has two outputs, the first is the top dead centre (TDC) index signal with a resolution of 1 pulse per revolution. The second is the crank angle degree marker (CDM) with a resolution of 1 pulse each 0.2 degree. Since the engine is 4-stroke, the encoder gives as output two TDC signals per cycle.

A quartz pressure transducer is installed into the spark plug in order to measure the in-cylinder pressure with a sensitivity of 19 pC/bar and a natural frequency of 130 kHz. It follows that a resolution of about 0.06 crank angle (CA) degrees is obtained at the engine speed of 1500 rpm. The in-cylinder pressure, the rate of heat release and the related parameters are evaluated on an individual cycle basis and/or averaged over 400 cycles [6].

New and advanced concepts and technical solutions are implemented in the injection system used in the present experiments to achieve single and multiple injection strategies. In particular, a fast electronic driver for the improved solenoid injector allows achieving a stable and consistent control of small injected quantities (±5% at 1mm^3/stroke) and reducing the dwell time between consecutive injections, with benefits on the engine performance and emissions.

All experiments are made by measuring in-cylinder pressure, exhaust emissions and performance in terms of indicated mean effective pressure high (IMEPH) and coefficient of variance of IMEPH (COV IMEPH). In particular, steady-state measurements of CO, CO_2, O_2, UHC (unburned hydrocarbons) and NO_x are performed in the raw exhausts by means of commercial analysers. CO, CO_2 and UHC are measured by non-dispersive infrared detectors (NDIR); NO_x and O_2 are detected through electrochemical sensors. An opacimeter is also employed to measure smoke emissions

Optical apparatus

The injection and combustion phases are analysed through an optical access on the engine head, as reported in figure 1. A customised protective case for an endoscopic probe, equipped with an optical sapphire window (5 mm diameter), is installed in the engine head of the 4th cylinder. This system allows investigating an area including the spark and the gasoline spray through an endoscope exhibiting a viewing angle of 70°. The field of view is

centred in the combustion chamber perpendicularly to the plane identified by the axes of the cylinder and of the injector, hence perpendicular to the plane of tumble motion.

Imaging measurements from ultraviolet (UV) to visible are performed by means of the optical experimental set-up shown in figure 1. The endoscopic probe is coupled with two high spatial and temporal resolution CCD cameras. The first is an intensified cooled CCD camera (ICCD). It is equipped with a 78 mm focal length, f/3.8 UV Nikon objective. The ICCD has an array size of 512x512 pixels and a 16-bit dynamic range digitization at 100 kHz. The optical assessment allows a spatial resolution of approximately 0.19 mm/pixel. Its spectral range spreads from UV (180 nm) until visible (700 nm). The ICCD operates at a digitizer offset of about 230 counts, but the dark noise fluctuation in the background is much smaller, less than 50 counts. Dark noise and photon statistical noise are both small compared with the measured intensity. The gasoline injection phase is characterized through the ICCD camera and an intense strobe lamp, which is introduced in the spark location through an optical fibre.

Table II reports the main data relevant to the operating condition taken under examination within the present work, including the duration of injection (DOI), the start of injection (SOI) and the CA of start of spark (SOS).

For all the optical measurements, the synchronization between the cameras and the engine is made by the crank angle encoder signal through a unit delay. More details are reported in ref.[7]

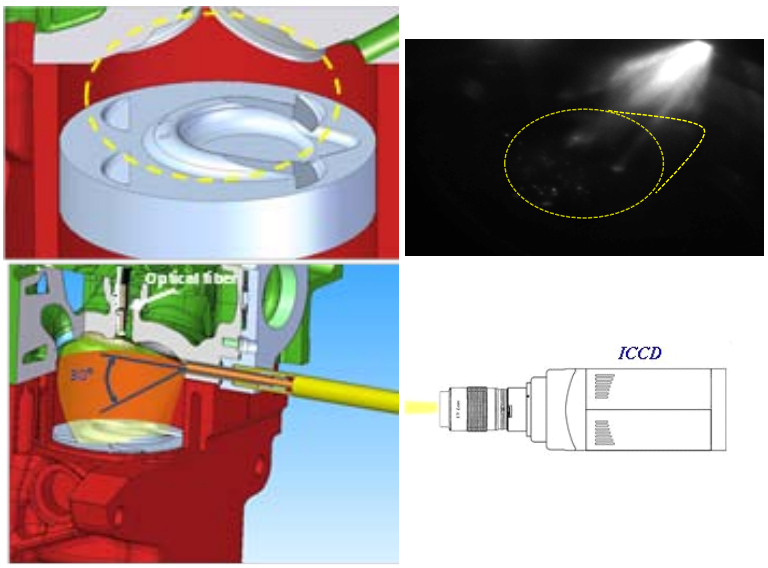

Figure 1 Sketch of the experimental set-up for optical investigation and detail of the combustion chamber: ICCD for UV-Visible measurements.

Table II Engine operating condition investigated at 1500 rpm (medium load)

Condition	DOI [CA]	SOI [CA]	SOS [CA]	P_{cyl} @ SOI [MPa]	IMEP [MPa]	COV IMEPH [%]	P_{inj} [MPa]
Stratified gasoline	14.8°	647°	707°	0.218	0.67	1.51	15

Experimental Characterisation of the GDI Injector

The injector mounted on the considered engine is a mini-sac seven-hole Bosch HDEV 5.1 with solenoid actuation. It is characterized by a hole diameter of 0.179 mm and by a static flow rate of 13.7 g/s at the injection pressure of 10 MPa. The injector exhibits a great flexibility to range from low to high load engine conditions.

The experimental campaign devoted to the injector characterization consists of both measurements of the delivered instantaneous mass flow rate and of images acquisition of the sprays issuing in an optically accessible vessel containing nitrogen under controlled conditions of temperature and pressure (298 K and 0.1 MPa, respectively).

Commercial gasoline is used (ρ=740 kg/m^3), within all the experimental campaign, as delivered by a hydropneumatic injection system without rotating organs. The injection system and the synchronized image acquisition set-up are managed by a programmable electronic control unit (PECU). This is an open system able to reproduce the injector energizing currents for the desired strategy in terms of number of injection pulses, durations, rise and dwell times. The PECU reproduces as an output a TTL (transistor transistor logic) signal, related to the injection event, for synchronizing the consecutive images management and acquisitions.

The gasoline mass flow rate is measured by means of an AVL Fuel Injection Gauge Rate System working on the Bosch tube principle [8, 9]. Figure 2 shows the relation between the solenoid energizing current profile and the corresponding fuel injection rate measured by the AVL Meter at the injection pressure of 15.0 MPa and for an energizing time of 1.46 ms. A delay of 0.35 ms is observed between the electronic SOI instant and the first appearance of gasoline droplets into the vessel while the negative peak at the nozzle closure, with the subsequent dumped oscillations, are imputable to inner fluidynamic effects [10]. The total amount of injected fuel is equal to 26.21 mg/str.

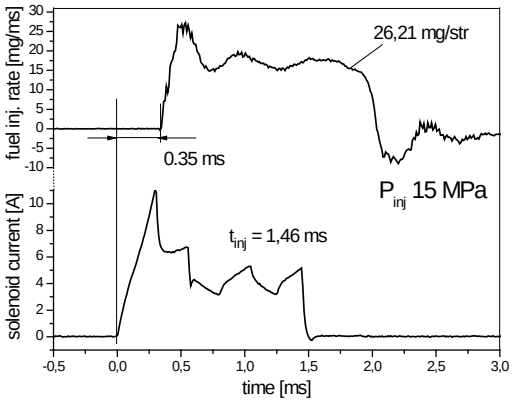

Figure 2 Solenoid energizing current and fuel injection rate.

The fuel has been sprayed in an optically-accessible vessel controlled in pressure and temperature. The injector command has been generated by a Programmable Electronic Control Unit managing its injection pressure, time-duration and kind of strategy. A synchronized pulse started both the flash enlightening and the shutter of a high-resolution CCD camera (1376x1040 pixels, 12 bit resolution, 0.5 μs shutter time). Images of the spray are so collected at different instants from the SOI. An overview of the experimental scheme for the image acquisition is reported in ref. [11]. The captured images are processed off-line by means of a proper software, able to extract the parameters characterizing the spray dynamics, namely penetration length and cone angle of one of the seven jets compounding the spray. Due to the high reproducibility and regularity of the jet evolution, a set of 5 images for each injection condition has been enough for a reliable extraction of the jet parameter with a good statistical analysis of the cycle-to-cycle dispersion. The images processing analysis is carried out in different steps: image acquisition and background subtraction, filtering, fuel spray edges determination and tip penetration measurements. Background subtraction and median filter procedures are adopted during the image acquisition to remove impulse noise and stray light, so to maintain sharp the spray edge. This is determined by selecting an intensity threshold level for separating the fuel region from the background ambient gas. More details about the image post-processing procedure can be found in ref. [9].

Numerical Simulation of the GDI Spray Dynamics

The 3D sub-model able to simulate the dynamics of the gasoline spray issuing from the considered injector is developed in the context of the software AVL Fire™ [12], in such a way to preliminary simulate the experiments devoted to the spray characterisation within the optically accessible vessel. Experimentally measured cone angles and injected mass flow rates are assumed as input variables for the model, whereas the measured penetration length serves as term of comparison for its calibration. The followed approach is the classical coupling between the Eulerian description of the gaseous phase and the Lagrangian description of the liquid phase as representative parcels (particles). A parcel consists of a number of droplets and it is assumed that all the droplets within one parcel have the same physical properties and behave equally when they move, break-up, coalesce, hit a wall or evaporate. The coupling between the liquid and the gaseous phases is made through source terms representing the exchange of mass, momentum and energy. In particular, the effect of turbulent dispersion on the droplets motion is treated following the sub-model by Gosman and Ioannides [13], coalescence with the sub-model by O'Rourke [14], evaporation with the sub-model by Dukowitz [15], wall interaction with the sub-model by Kuhnke [12], droplet break-up with the sub-model by Huh-Gosman [16].

Main novelty of the present approach lies in the definition of the droplets size at the nozzle exit section, considered variable according to a probabilistic log-normal distribution whose expected value is assumed as coincident with the following theoretical diameter:

$$D_{th} = C_d \left(\frac{2\pi\tau_f}{\rho_g u_{rel}^2} \right) \lambda^* \tag{1}$$

being τ_f the gasoline surface tension, ρ_g the surrounding gas density, u_{rel} the relative velocity between the fuel and the gas, C_d a constant of the order of the unity (indeed taken equal to the unity), and the parameter λ^* deriving from the hydrodynamic stability analysis and indicating the dimensionless wavelength of the more unstable perturbation to the liquid-gas interface at the injector exit section. The variance of the distribution, σ, is a parameter of the sub-model to be properly tuned. A further parameter to be assessed in the phase of tuning is the constant C_1 regulating the aerodynamic break-up time in the Huh-Gosman sub-model. An automatic procedure is developed to define the values of these two constants, consisting in the solution of a single objective optimization problem minimizing the error between the results of the numerical computations and the experimentally measured penetration length. In other words, instead of resorting to a search of the values of the constants by trial and error, i.e. for successive approximations, as made by authors in ref. [4], an optimization problem is set-up, where the Simplex algorithm is used to assure a high "portability" of the model, namely a good prediction capability, as the injector operating conditions are varied. At each injection pressure, the log-normal distribution of the initial droplet size at the injector exit section is built starting from a certain value of σ and the value of the expected value computed according to eq. (1). The distribution profile is transferred to the Fire™ spray sub-model, that also uses a certain value of C_1. The model realizes the spray computation in the interval of time needed to inject a given mass of gasoline (according the experimental measurements), and furnishes, as an output, the penetration length of the jets compounding the spray. The error between the numerically computed penetration length, as averaged over the six (or seven) jets, and the experimentally measured one is minimized by the Simplex algorithm. The objective function is defined as :

$$Obj\big|_{\sigma,C_1} = \sum_{i=1}^{n} \left[l_{ex}(t_i) - l_{num}(t_i) \right]^2 \tag{2}$$

where n represents the number of discrete instants of time in which the injection interval of time is subdivided, t_i is the i^{th} instant of time, and $l_{ex}(t_i)$ and $l_{num}(t_i)$ the values, respectively, of the experimentally measured and the numerically computed penetration length at t_i. The experimentally measured penetration length, indeed, is evaluated by means of a smoothing spline passing through the actual measurements points in the time-length plane. Some results of the developed spray model are synthetized in figures 3 and 4. In figure 3 the comparison between the experimentally measured penetration length (of one of the seven jets compounding the spray) and the numerically computed one (as averaged over the seven jets) is reported for four different injection pressures. The choice to refer to an average of the numerical data is made to neglect the jet-to-jet variation. From the experimental point of view, insulating a single spray allows a more reliable measurement of the penetration length.

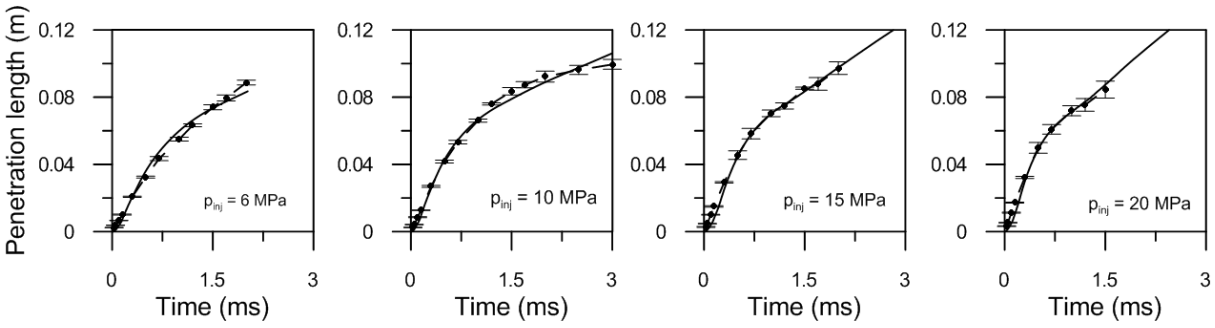

Figure 3 Numerical (continuous line) and experimental (dashed line with dots) penetration lengths of the GDI spray in a confined vessel at various injection pressures.

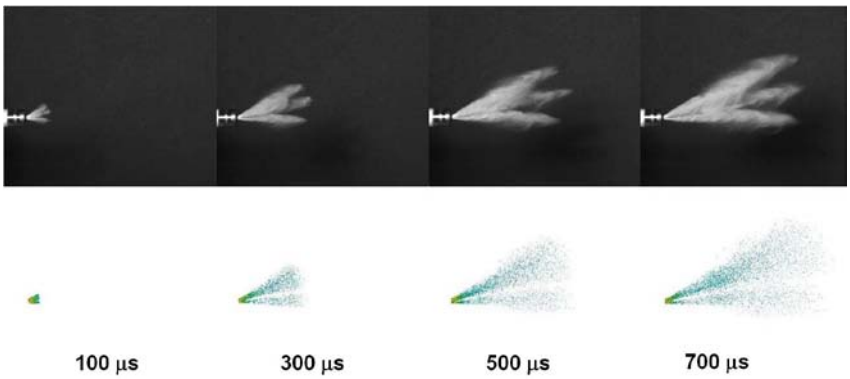

Figure 4 Experimentally collected (top) and numerically computed (bottom) images of the spray at the injection pressure of 15 MPa.

The spray structure is represented in figure 4, that shows experimental images and numerically computed sprays at various instants of time from the start of injection (SOI) at the injection pressure of 15 MPa. Slight differences appear in the spray tip shape that is sharper in the experiments. This discrepancy can be reduced by further adjusting the far filed break-up characteristic time of droplets, although it is to be considered that, at the distance from the nozzle where the differences become appreciable, the effect of evaporation should be also taken into account. Neglecting evaporation during the model validation, on the other hand, may be considered as sufficiently accurate due to the fact that the exchange of mass between the liquid and the gas phase occurs as superimposed to the droplets break-up, that represents the preponderant phenomenon leading to mixture formation.

The 3D Engine Model

The spray model described in the previous section is employed within a 3D numerical model able to simulate the thermo-fluidynamic processes occurring within the cylinder and intake and exhaust ducts of the considered GDI engine. The engine model is also developed within the AVL Fire™ environment.

The discretization of the computational domain is made through a home-made procedure, instead than resorting just to the pre-processing software included in the Fire™ graphical user interface (GUI), namely the fame engine plus (FEP) module [4, 12]. The search for a compromise between accuracy of results and low calculation time, indeed, led to assess a "customized" methodology for the grid design. The main aspect of this methodology is the construction of a block structure grid. As an example, the volume surrounding the valves is built by rotation of a regular 2D properly designed grid to generate only hexahedral cells. Figure 5.a shows the intake valve, with its surrounding volume, and the coupling with the grid relevant to the intake duct. The discretization of the volume surrounding the spark plug, hence the electrode, is instead shown in figure 5.b, together with its coupling with the combustion chamber volume. The FEP is used for the construction of both the computational subdomains, but the separation into two parts allows a better control of the cells size and regularity. The number of cells is varied during the computation to avoid excessive distortion from 160000 at the top dead centre in the closed valve period to 340000 for the intake stroke or 420000 for the exhaust stroke. These numbers refer to half the domain. The condition of symmetry with respect to the cylinder axis, in fact, is exploited.

The charge turbulent motion is modelled through the k-ζ-f model, the combustion process according to the ECFM model [14]. NO formation follows the extended mechanism formulated by Zeldovich. A semi-empirical model for soot formation is also considered. Finally, it is to be pointed out that in the application of the spray model to the simulation of the GDI engine working cycle, spray-wall interaction is also taken into account. The impingement of the spray on the engine walls gives rise to the deposition of a liquid film on the walls and to a secondary atomization of the impacting droplets. The process is strongly affected by the conditions of pressure, velocity and temperature of the surrounding gas and by the value of the wall temperature. These aspects are treated within the “wallfilm” module of the Fire™ code, that involves the Kuhnke model [12]. Boundary conditions for the 3D model are derived from a preliminary 1D analysis of the entire propulsion system. Initial conditions are set according to the experimental data. The computation is initiated at the crank angle of TDC, some degrees before the intake valves opening (IVO).

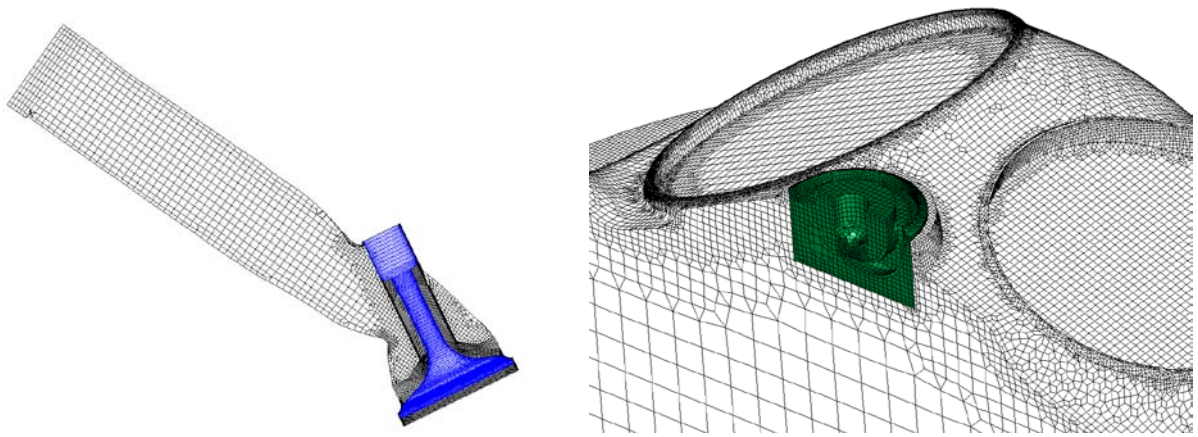

(a) (b)

Figure 5 Two particulars of the computational domain.

The whole engine cycle is simulated. A preliminary validation phase, whose details are here not reported for the sake of brevity, regarded the computation of a motored pressure cycle, the check about the repeatability of

results obtained over more than one computational cycle (necessary due to the kind of imposed initial conditions) and a check about the grid invariance of the obtained results.

The comparison between the experimentally measured and the numerically computed pressure cycles is reported in figure 6 for the medium-speed, medium-load condition reported in Table II. The results are obtained after a validation phase regarding, in particular, the combustion model, hence the choice of the constants regulating the the transfer of fuel from the pure fuel zone to the mixed zone and the flame stretch factor. Both the intake stroke and the compression stroke are quite well reproduced. The combustion phase is also in good agreement.

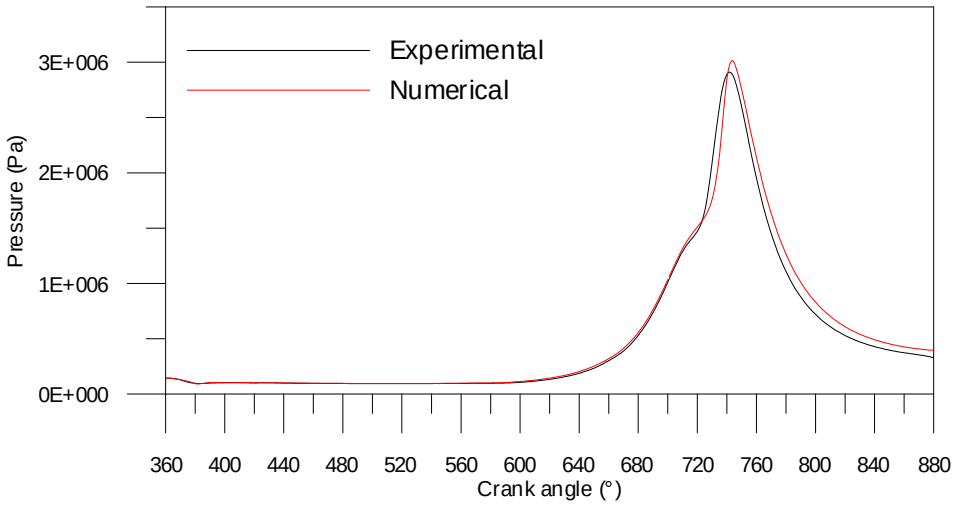

Figure 6 Comparison between the experimentally collected and the numerically computed pressure cycles.

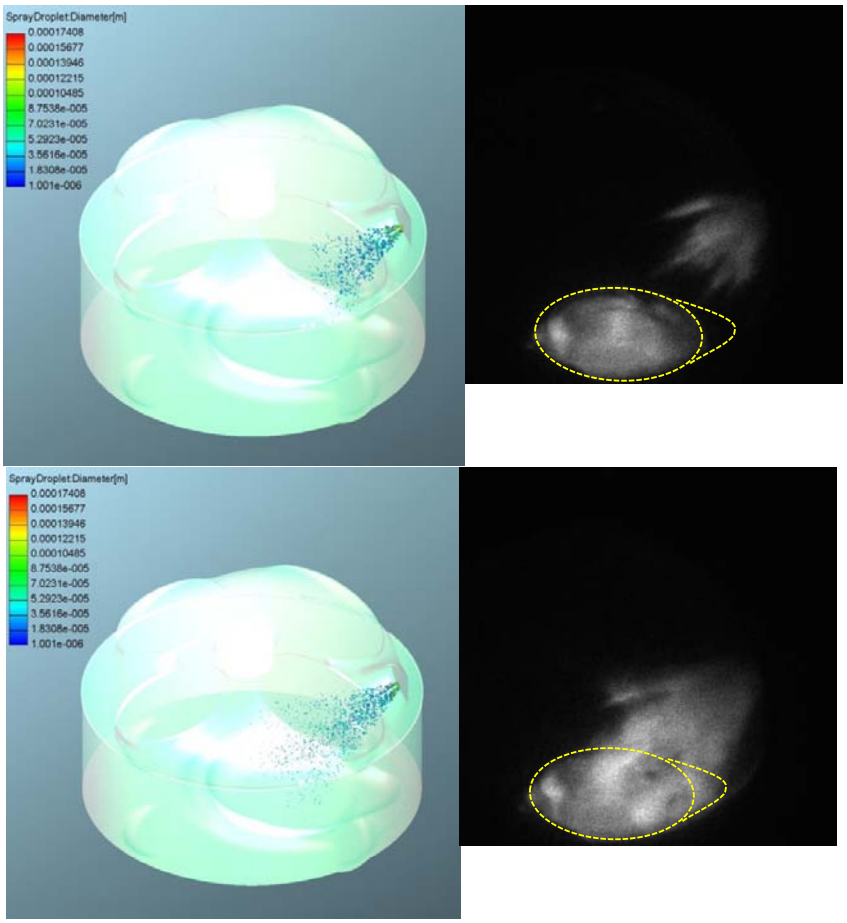

Figure 7 Numerically computed spray evolution and experimentally collected images 3° (top) and 5° after SOI (bottom).

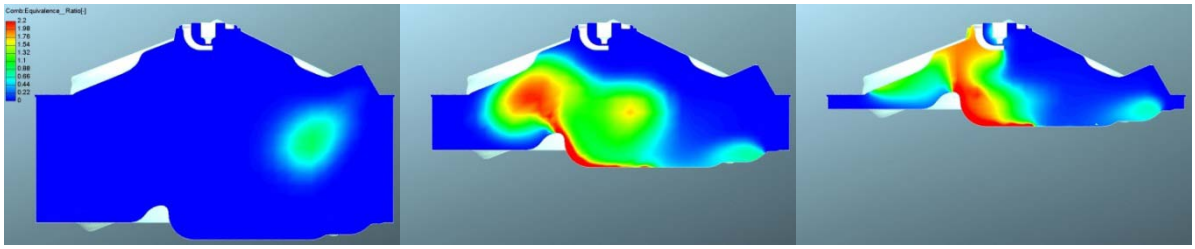

Figure 8 Numerically computed equivalence ratio on a plane passing through the spark location images 4°after SOI (left), 30° after SOI (centre) and at the CA of SOS (right).

Information concerning the spray evolution can be deduced from figure 7, where the comparison between the numerically computed spray and the experimentally collected images of the spray within the engine is made for two values of CA, namely 3° and 5° after SOI.

An idea of the gasoline vapour distribution within the combustion chamber is given in figure 8, where a sequence of drawings is shown representing the equivalence ratio distribution on a plane passing through the spark plug axis at three different values of CA, namely 4° after SOI, 30° after SOI and at the time of Start Of Spark. The charge is not homogeneous, but stratified, due to the late start of the injection event during the working cycle, that completely occurs during the compression stroke.

Conclusions

Mixing control is fundamental in internal combustion engines. It assures flame stability, reduction of pollutants, improved combustor efficiency, reduced combustor size and greater combustor lifetimes.

Achievement of optimal charge conditions at all the engine loads and speeds in modern gasoline GDI SI engines is undoubtedly a challenging task, especially if the so-called mixed mode boosting is to be realized, with homogeneous stoichiometric or rich mixtures at the higher loads, and stratified lean mixtures at the lower ones. This is the reason why fully automatic procedures to be used in the phase of definition of the engine governing parameters are strongly demanded.

Present work aims at presenting a 3D numerical model able to reproduce the in-cylinder processes of a high performance GDI engine. The model includes a sub-model for the spray dynamics tuned through an automatic procedure on the ground of an experimental campaign conducted in an optically accessible vessel.

The developed 3D engine model well reproduces the in-cylinder thermo-fluidynamic process and may be included within a multi-objective optimization tool to optimize the engine performance by proper choice of the injection strategy and the time of spark ignition.

References

[1] Alkidas, A. C., *Energy Conversion and Management* 48: 2751–2761 (2007).
[2] Patent N° 7415348 B1 - Multiple Injection Blend For Direct Injected Engines Assignee: GM Global Technology Operation, Inc. Detroit, MI (US), 2008.
[3] Carling, R. W., *Predictive Simulation of Combustion Engine Performance in an Evolving Fuel Environment*, Sandia National Laboratories, 2010.
[4] Costa, M., Sorge, U., Allocca, L., *Energy Conversion and Management* 60: 77-86 (2012).
[5] Malaguti, S., Fontanesi, S., Vaglieco, B. M., Sementa, P., Catapano, F., SAE Paper 2011-24-0031, 2011.
[6] Zhao, H., Ladommatos, N., *Engine Combustion Instrumentation and Diagnostics*, SAE Int. Inc, 2001.
[7] Sementa, P., Vaglieco, B.M., Catapano, F., *Fuel* 96: 204-219 (2012).
[8] Bosch, W., SAE Paper 6607496, 1966.
[9] Wallace, I., *Injection Rate Gauge: Pass Off Information and User Instructions - Fuel & Engine Management Systems*, Graz, 2002.
[10] White, F.M., *Fluid mechanics*, Mc Graw Hill, 1986.
[11] Alfuso, S., Allocca, L., Caputo, G., Corcione, F.E., Montanaro, A., Valentino, G., SAE Paper 2005-24-9, 2005.
[12] AVL Fire™ v2009 Users Guide - ICE Physics & Chemistry.
[13] Gosman, A. D., Ioannides, E., *J. Energy* 7: 482-490 (1983).
[14] O'Rourke, P.J., IMechE - Stratified Charge Automotive Engines Conference, 1980.
[15] Dukowicz, J. K., Los Alamos Report LA-7997-MS, 1979.
[16] Huh, K. Y., Gosman A. D., International Conference on Multiphase Flows 1991, Japan, 1991.